Journal Pre-proof

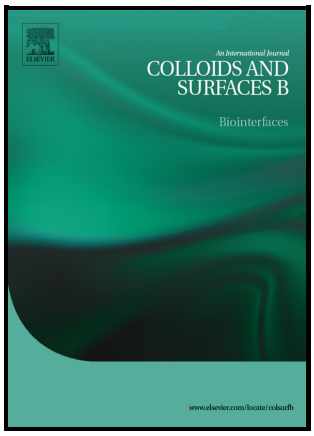

Nanoparticles of nucleotide-free analogue of vitamin B_{12} formed in protein nanocarriers and their neuroprotective activity in vivo

Larissa A. Maiorova, Olga A. Gromova, Ivan Yu. Torshin, Tatiana V. Bukreeva, Tatiana N. Pallaeva, Boris V. Nabatov, Ilia A. Dereven'kov, Yurii A. Bobrov, Andrei A. Bykov, Vadim I. Demidov, Alla G. Kalacheva, Tatiana E. Bogacheva, Tatiana R. Grishina, Elena D. Nikolskaya, Nikita G. Yabbarov

PII: S0927-7765(24)00424-7

DOI: https://doi.org/10.1016/j.colsurfb.2024.114165

Reference: COLSUB114165

To appear in: *Colloids and Surfaces B: Biointerfaces*

Received date: 7 April 2024
Revised date: 16 August 2024
Accepted date: 17 August 2024

Please cite this article as: Larissa A. Maiorova, Olga A. Gromova, Ivan Yu. Torshin, Tatiana V. Bukreeva, Tatiana N. Pallaeva, Boris V. Nabatov, Ilia A. Dereven'kov, Yurii A. Bobrov, Andrei A. Bykov, Vadim I. Demidov, Alla G. Kalacheva, Tatiana E. Bogacheva, Tatiana R. Grishina, Elena D. Nikolskaya and Nikita G. Yabbarov, Nanoparticles of nucleotide-free analogue of vitamin B_{12} formed in protein nanocarriers and their neuroprotective activity in vivo, *Colloids and Surfaces B: Biointerfaces,* (2024) doi:https://doi.org/10.1016/j.colsurfb.2024.114165

Nanoparticles of nucleotide-free analogue of vitamin B_{12} formed in protein nanocarriers and their neuroprotective activity in vivo

Larissa A. Maiorova[1,2*], Olga A. Gromova[2], Ivan Yu. Torshin[2], Tatiana V. Bukreeva[3], Tatiana N. Pallaeva[3], Boris V. Nabatov[3], Ilia A. Dereven'kov[1], Yurii A. Bobrov[4], Andrei A. Bykov[4], Vadim I. Demidov[5], Alla G. Kalacheva[5], Tatiana E. Bogacheva[5], Tatiana R. Grishina[5], Elena D. Nikolskaya[6], Nikita G. Yabbarov[6]

[1]Institute of Macroheterocyclic Compounds, Ivanovo State University of Chemistry and Technology, Ivanovo, Russia

[2]Federal Research Center Computer Science and Control of Russian Academy of Sciences, Moscow, Russia

[3]Kurchatov Complex Crystallography and Photonics, National Research Centre "Kurchatov Institute", 123182, Moscow, Russia

[4]NT-MDT Spectrum Instruments, Moscow, Zelenograd, Russia

[5]Ivanovo State Medical University, Ministry of Health of Russia, Ivanovo, Russia

[6]N.M. Emanuel Institute of Biochemical Physics of Russian Academy of Sciences, 4 Kosygina Street, 119334 Moscow, Russia

* Corresponding author.

E-mail: maiorova.larissa@gmail.com (Larissa A. Maiorova)

Abstract

Recently, we have described the first supermolecular nanoentities of vitamin B_{12} derivative, viz. monocyano form of heptabutyl cobyrinate, unique nanoparticles with strong noncovalent intermolecular interactions, emerging optical and catalytic properties. Their nearest analogue, heptametyl cobyrinate (ACCby), exhibits bioactivity. Here, we demonstrate the first example of the formation of nanoparticles of this nucleotide-free analogue of vitamin B_{12} in protein

nanocarriers and neuroprotective activity in vivo of the own nanoform of the drug. The preparation and characterization of nanocarriers based on bovine serum albumin (BSA) loaded with vitamin B_{12} (viz. cyano- and aquacobalamins) and ACCby were performed. Nucleotide-free analogue of vitamin B_{12} is tightly retained by the protein structure as well and exists in an incorporated state in the form of nanoparticles. The effect of encapsulated drugs on the character and severity of primary generalized seizures in rats induced by the pharmacotoxicant thiosemicarbazide was studied. Cyanocobalamin and ACCby exhibited a neuroprotective effect. The best influence of the encapsulation on the effectiveness of the drugs was achieved in the case of ACCby, whose bioavailability as a neuroprotector did not change upon introduction in BSA particles, i.e., 33% of surviving animals were observed upon ACCby administration in free form and in encapsulated state. No surviving rats were observed without the administration of drugs. Thus, BSA nanocarriers loaded by nanoparticles of nucleotide-free analogues of vitamin $B_{12,}$ including hydrophobic ones, can be recommended for neuroprotection and targeted delivery.

Keywords:

vitamin B_{12} derivatives; bovine serum albumin; nanocarriers; nanoparticles, neuroprotective properties; thiosemicarbazide

1. Introduction

Vitamin B_{12} is a necessary component for human metabolism involved in methylation of homocysteine and isomerization of methylmalonyl-CoA [1]. Cyanocobalamin (CNCbl; Fig. 1A) is used to treat megaloblastic anemia, disorders of nerve myelination, liver pathology, etc. Aquacobalamin (H_2OCbl) shares the same functions as CNCbl and additionally can be used as cyanide antidote binding cyanide to form nontoxic CNCbl [2]. Diaquacobinamide, a nucleotide-free derivative of H_2OCbl, acts as an antidote of cyanide [3], hydrogen sulfide [4], and methyl mercaptan [5], as well as strong antioxidant [6]. The development of new effective

pharmaceuticals based on vitamin B_{12} [7], including semi-synthetic derivatives [8-10], and the study of their pharmacological activities using nanoengineering carriers are promising directions of modern pharmacology and biomedicine.

Within nanopharmaceutics, i.e., the application of nanotechnology to the preparation of drug formulations, the development of methods for "targeted" delivery of vitamin B_{12} (e.g., to neurons, hepatocytes, etc.) is of great importance. Encapsulation of vitamin B_{12} allows to reduce vitamin losses in the presence of oxidizing agents and ensure delivery of the vitamin to target tissues using proper selection of capsule properties. Previously, we successfully encapsulated vitamin B_{12} in nanoengineered micron-sized polymer capsules [11]. Within the capsules, the compound exists in the form of nanostructures. The formation of molecular assemblies at the interfaces is a specific feature of this class of compounds [12–15]. Similar mono- and heteromolecular nanostructures containing drugs can be prepared *in vitro* [16-20] with subsequent introduction into the body for a therapeutic effect or form spontaneously when molecular solutions are introduced. Self-assembly is a key player in materials nanoarchitectonics [21-28]. Supramolecular polymers have been created using diverse self-assembly strategies wherein biomolecules are employed [29,30]. The possibility of the self-assembly of compounds into 2D and 3D nanostructures possessing controlled properties was demonstrated [31-34]. Recently, we have reported the formation in this way of supermolecular nanoentities (SMEs) of vitamin B_{12} derivative (viz. heptabutyl ester of aquacyanocobyrinic acid, $AC^{Bu}Cby$), i.e., unique nanoparticles exhibiting strong non-covalent intermolecular interactions and possessing intriguing properties [35]. Besides reproducing the functional properties of vitamin B_{12} complexes with proteins in living organisms, the nanoparticles demonstrate important advantages over vitamin B_{12}. They are more effective in oxygen reduction/evolution reactions and in transformations into other forms [35]. Such nanoparticles can become an alternative form of drugs widely used in medicine (in particular, vitamin B_{12}).

In addition to nanoengineered polymer capsules, protein particles, in particular albumin particles, could be promising carriers due to their excellent biocompatibility, wide biodegradation possibilities and versatile functionalities [36-38]. Serum albumin is the most abundant protein in plasma. It is a key player in enhancing the bioavailability and regulating the transport of long-chain fatty acids, nutrients and metal ions, as well as a variety of systemically administered drugs [39], by increasing their bioavailability and stability in biological fluids [40,41]. Its natural properties as a blood transporter widen up the perspective of albumin loading and/or conjugation with various therapeutic payloads to enhance their pharmacokinetics.

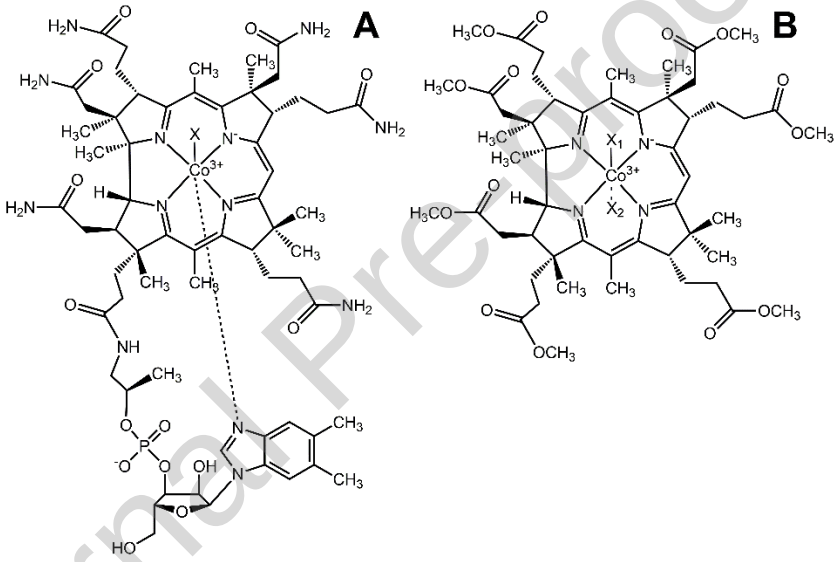

Fig. 1. Structures of vitamin B_{12} (A; cobalamins, X = CN^-, H_2O and others) and its nucleotide-free analogue (B; heptamethyl ester of aquacyanocobyrinic acid $X_{1,2}$ = H_2O, CN^-)

Comparative chemoreactome modeling of biological properties of CNCbl and its derivatives (H_2OCbl, heptamethyl ester of aquacyanocobyrinic acid and stable yellow corrinoid) showed that these compounds are not toxic and may exhibit neuroprotective effects [42]. We indicated that a semi-synthetic slightly hydrophobic derivative of vitamin B_{12} (heptamethyl ester of aquacyanocobyrinic acid, ACCby; Fig. 1B) exhibits biological activity in vivo [43]. The investigation of the properties of these compounds incorporated into protein nanocarriers represents considerable interest. As the material of carriers, bovine serum albumin (BSA) can be

used. Note that reactions of vitamin B_{12} and its derivatives with BSA have been investigated in depth [44-47]. In particular, H_2OCbl and ACCby form complexes with BSA predominantly via lysine side chains; however, the binding occurs relatively weakly [44,45], which makes the loading of BSA molecules by these complexes inefficient. The loading of vitamin B_{12} or its derivatives may be improved by using semi-artificial BSA particles.

This work was aimed at the fabrication of BSA-derived submicron particles containing vitamin B_{12} (in cyano and aqua-forms) and its nucleotide-free analogue and the characterization of their properties, including the state of the drug and its interaction with the carrier. In particular, an extensive investigation of the characteristics of the BSA particles was performed by SEM, AFM and absorption spectroscopy methods, and their biological properties were evaluated. The toxicity of nucleotide-free derivative of vitamin B_{12} and BSA particles containing the derivative was tested on fibroblasts. Using a model of thiosemicarbazide-induced seizures in rats, the pharmacological effects of nanocarriers with these compounds were assessed, including histological analysis and comparison of the therapeutic effect of drugs upon administration in BSA carriers and in free state.

2. Materials and methods

2.1. Materials

Cyanocobalamin (≥ 98%; Sigma-Aldrich), hydroxocobalamin hydrochloride (≥ 96%; Sigma-Aldrich), bovine serum albumin (heat shock fraction, pH 5.2; ≥ 96%; Sigma-Aldrich), 0.9% sodium chloride solution (Escom NPK, Russia), phosphate saline buffer solution (Amresco) were used as received. Heptamethyl ester of aquacyanocobyrinic acid was synthesized according to reported procedure [45].

2.2. Fabrication of BSA particles

20 ml of $CaCl_2$ solution containing 20 mg of bovine serum albumin was stirred in a 100 ml beaker for 1 min. Then 20 ml of Na_2CO_3 was quickly added with vigorous stirring for 30 s at room temperature. The resulting protein/$CaCO_3$ particles were separated by centrifugation at 3000 × g for 3 min and washed twice with 0.9% NaCl solution. The particles were suspended in a solution of glutaraldehyde (GA) (final concentration 0.1%) and incubated at room temperature for 1 h, followed by centrifugation at 3000 × g for 3 min. The remaining unbound GA groups in the particles were reduced using $NaBH_4$, and then the $CaCO_3$ matrix was removed by treatment with a solution of ethylenediaminetetraacetic acid (EDTA) (0.25 M, pH 7.4) at room temperature for 30 min. The resulting protein particles were centrifuged, washed 3 times, and resuspended in saline for further use.

2.3. Encapsulation of vitamin B_{12} and its derivatives into the BSA particles and release

The equal volumes (250 µl) of the BSA particles were incubated in the aqueous solution of CNCbl or H_2OCbl and in ACCby ethanol solution (≈ 5 mM). After stirring for 2 hours, the particles were isolated by centrifugation and the supernatant was analyzed by spectroscopy.

Quantities of complexes incorporated into protein particles were determined spectrophotometrically (using absorption values at 361, 350 and 365 nm for CNCbl, H_2OCbl and ACCby, respectively). The loading capacity was determined as the ratio of the mass of the encapsulated substance (mg) to the total mass of particles used during sorption.

To determine the release of substances from protein particles, samples were placed in test tubes with saline solution and incubated on a shaker (1000 rpm, IKA MS 3 basic) to prevent sedimentation. After certain periods of time the tubes were removed from the shaker, the suspension was centrifuged (1 min, 5000 rpm), and the supernatant was collected for spectrophotometric study. To determine the release of substances in the presence of pronase, 100 µl of pronase solution (1.7 mg/ml) was added to an aliquot of particles (100 µl).

2.4. Methods employed for investigation of BSA nanocarriers

The particle size distribution and ξ-potential were investigated by dynamic light scattering (DLS) using a Zetasizer Nano ZS (Malvern Instruments). The size value was calculated from eight independent measurements (20 consecutive measurements for each determination). The ξ-potential was evaluated from five consecutive measurements.

Analysis of the size, shape and surface morphology was carried out using VEGA 3 SBH (TESCAN, Czech Republic) and JSM-7401F (JEOL) at a voltage of 5 kV in the secondary electron detector mode scanning electron microscopes.

UV-vis spectra of solutions were recorded using Shimadzu UV-1800 spectrophotometer. Lambda 650 Perkin Elmer spectrophotometer was used to determine loading and release of complexes from BSA particles. UV-vis spectra of loaded particles were recorded using Cary 5000 (Varian) spectrophotometer with DRA-2500 integrating sphere. 10 mm fluorimeter quartz cuvettes were used.

AFM images were acquired with the Ntegra probe microscope of the NTMDT-SI company. NSG01 probes with a resonant frequency of 125-160 kHz and an elastic stiffness of 6.3-14 N/m were used. The scanning was performed in semi-contact mode with a frequency of 0.3-1 Hz.

Differential scanning calorimetry (DSC) experiments were carried out on a Netzsch STA 449F1 synchronous thermal analyzer in platinum crucibles with pierced lids. The samples were heated in an air atmosphere at a rate of 15 K/min.

2.5. Cell Culture

The immortalized human fibroblasts BJ-5ta cell line was maintained in 25 cm^2 polystyrene flasks in the DMEM medium supplemented with 10% FBS and gentamycin (50 μg/ml) at +37°C in a humidified atmosphere containing 5% CO_2. The cells were replated using trypsin-EDTA solution twice per week.

2.6. Cytotoxic Activity Analysis

BJ-5ta cells were seeded in 96-well plates (3000 cells per well) 24 h before the experiment and incubated under standard conditions. The samples were added in triplets and then incubated under standard conditions for 72 h. Cells photo were taken at 1, 24, 48, 72 h of incubation by Nikon Diaphot phase contrast microscope at 40x magnification and a Levenhuk M1400Plus camera. We applied standard MTT assay to evaluate cells survival. Each well was supplemented with 50 µl of MTT solution (1 mg/ml) in the serum-free DMEM and incubated during 4 h. Next, the medium was aspirated, precipitated formazan crystals in each well were dissolved in 100 µl of DMSO, and the light absorption was measured at 540 nm using a microplate reader (Bio-Rad 680). Cell viability was determined as the percent of untreated control. Survival curves plotting, IC50 values calculation, and statistical analysis were performed in Excel (Microsoft Corporation, Redmond, WA, USA) and OriginPro (version 2020b, OriginLab Corp., Northampton, MA, USA).

2.7. Cytotoxic activity (Annexin V - FITC/PI staining)

The following samples were used throughout the experiments: C - control cells; 1 – ACCby (0.04 and 0.2 mM); 2 – BSA particles loaded with ACCby (4.3 mg/ml, 0.87 mg/ml) (5% ACCby content); 3 – empty BSA particles (4.3 mg/ml, 0.87 mg/ml). Samples 2 and 3 were dissolved in culture medium, sample 1 was dissolved in DMSO to prepare stock solution.

50000 cells were cultured in 12-well plate in 1 ml of medium 24 h before the experiment. The next day, samples were added. Cells were stained with annexin V -FITC/PI after 48 and 72 h of incubation and were analyzed with DaKo CyAn ADP flow cytometer. Briefly, cells were detached after incubation with Trypsin-EDTA solution, washed 2 times with cold PBS and resuspended in 100 µl of binding buffer ($3 \cdot 10^5$ cells). 5 µl of Annexin V-FITC and 10 µl of PI solution were added to the cells suspension and incubated without light access for 15 min at room temperature. After incubation, 400 µl of binding buffer was added to the samples and analyzed using flow cytometer

(λ 488 nm excitation, 530/40 nm bandpass filter for FITC and λ 488 nm excitation, 613/20 nm bandpass filter for PI).

2.8. Neurological tests

The study was carried out on 24 white male rats weighing 200–300 g in accordance with "Rules of good laboratory practice" (Appendix to the order of the Ministry of Health of the Russian Federation No. 199n dated 04/01/2016) and allowed by the local ethical committee of Ivanovo State Medical University. During the studies, animals were kept under standard conditions in accordance with Directive 2010/63/EU of the European Parliament and of the Council of the European Union of 22 September 2010 concerning the protection of animals used in scientific studies. Indoor air control was in compliance with environmental parameters (temperature 18–26 °C, humidity 46–65%). The rats were kept in standard plastic cages with bedding; the cages were covered with steel lattice covers with a stern recess. The floor area per animal met regulatory standards. The animals were fed in accordance with Directive 2010/63/EU. The animals were given water ad libitum. The water was purified and normalized for organoleptic properties in terms of pH, dry residue, reducing substances, carbon dioxide, nitrates and nitrites, ammonia, chlorides, sulfates, calcium and heavy metals in standard drinkers with steel spout lids.

The study is based on a comparative study of 4 groups of observations. In the control group (represented by 6 rats), the animals were intraperitoneally injected with the physiological saline of BSA particles, then the model of primary generalized seizures caused by thiosemicarbazide was reproduced. In the 2nd, 3rd, and 4th groups (6 rats in each), animals were intraperitoneally injected with the physiological saline of cyanocobalamin, aquacobalamin, and hydrophobic derivative of vitamin B_{12} (ACCby) respectively, loaded BSA particles for 18 days, and on the 19th day they induced convulsions - thiosemicarbazide was administered at a dose of 28 mg/kg body weight.

2.9. Pathohistological studies

Sectional material was obtained by simultaneous decapitation of laboratory animals 90 minutes after the reproduction of primary generalized seizures. By means of craniotomy, the entire brain was removed and fixed in a 10% solution of neutral formalin; after 1 day, the area of the precentral gyrus of the forebrain, the cerebellum, and the brain stem were isolated using frontal incisions. After secondary fixation and washing of the material, wiring (dehydration) of the nerve tissue was carried out using 99% isopropyl alcohol. Subsequently, pieces of the brain were embedded in paraffin and histological sections 5-6 μm thick made on a Microm sled microtome were stained with hematoxylin and eosin. Duplicate sections were stained using the Biovitrum reagent kit using the Nissl method.

2.10. Statistical analysis

In cell analysis survival curves plotting, IC50 values calculation, and statistical analysis were performed in Excel (Microsoft Corporation, Redmond, WA, USA) and OriginPro (version 2020b, OriginLab Corp., Northampton, MA, USA). Graphs in “logarithm of concentration-viability” coordinates were analyzed by nonlinear methods in OriginPro-8 and IC50 was calculated first in μg/l, then in mmol/l. Morphometric analysis of structural changes in neurons was performed by direct counting of histological features.

For the studied parameters, the mean and standard deviation (M±S.D.) were calculated. Statistical analysis and the significance of other intergroup differences was estimated out using the Kruskal-Waliss-Dunn test (i.e., Kruskal-Wallis multiple comparison P-values with Bonferroni correction; applying the Kruskal-Wallis test to assess the statistical significance of differences in the medians of three or more independent groups, followed by Dunn's test). The differences were considered significant at a significance level of 0.05.

3. Results and discussion

3.1. Formation and characterization of BSA particles loaded by vitamin B_{12} (cyano- and aquacobalamins) and its nucleotide-free analogue (heptamethyl ester of aquacyanocobyrinic acid).

Figure 2A provides the scheme of BSA particles synthesis. Formation of calcium carbonate from calcium chloride and sodium carbonate in the presence of BSA leads to simultaneous trapping of protein molecules. Successive cross-linking of BSA molecules immobilized into $CaCO_3$ pores by glutaraldehyde allows to conserve shape and size of produced BSA particles after dissolution of inorganic matrix. Using this procedure, we prepared stable BSA particles with average diameter of 955 нм (PDI 0.448; Fig. S1). SEM images (Figs. 3A,B) indicate that the particles have elongated shape and can be easily dispersed in aqueous solutions due to existence in a non-aggregated state. The colloidal stability of the particles was evaluated by monitoring their size during storage at 4°C. Storage for 2 months resulted in a slight increase in size from 955 to 1080 nm, which could be attributed to insignificant aggregation of colloidally stable particles.

Next, vitamin B_{12} (CNCbl), its aqua-form (H_2OCbl), and its nucleotide-free analogue (ACCby) were adsorbed in BSA particles. Using UV-vis spectroscopy, we determined loading capacity of BSA particles, to be 0.026, 0.077 and 0.051 mg of complex per mg of BSA for CNCbl, H_2OCbl and ACCby, respectively. The lowest loading capacity of CNCbl compared to other species can be explained by its weak interaction with BSA matrix, i.e., it does not form coordination bonds with protein residues and aggregates or nanoparticles (vide infra). We determined values of zeta potential for surface of particles before and after loading complexes (Table 1). BSA particles in water (pH 6) exhibit slightly negative potential -9 mV that agrees with the zeta potential of free BSA, which has negative charge at physiological conditions [48]. Binding of vitamin B_{12} affects the value of zeta potential, whereas the changes of zeta potential are more pronounced in the case of incorporation of its aqua-form (-24 mV) and nucleotide-free analogue (-17 mV). These results indicate weak structural changes of BSA particles upon binding of cyano-form of vitamin B_{12} and high structural changes for complexation with its aqua-form and ACCby.

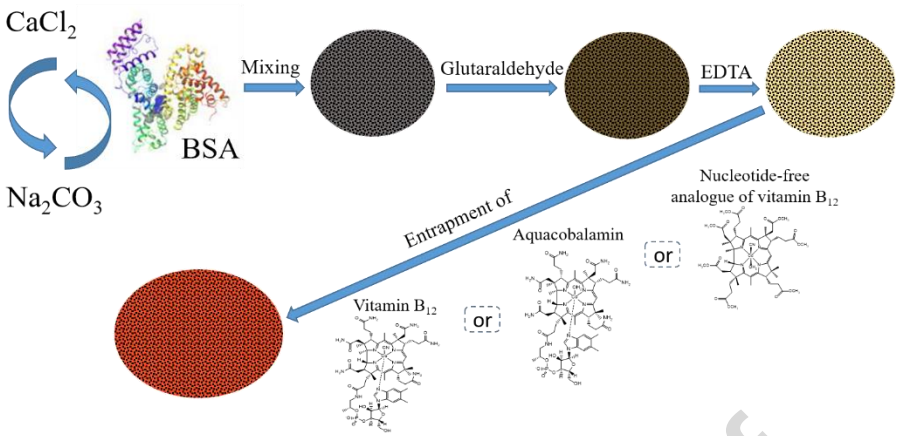

Fig. 2. Scheme of synthesis of BSA nanoparticles with subsequent loading of vitamin B_{12}, its aqua-form and nucleotide-free analogue.

Table 1. Values of zeta potential of BSA particles at pH 6

Sample	Zeta potential, mV
Empty BSA particles	-9
BSA particles + vitamin B_{12} (cyanocobalamin, CNCbl)	-14
BSA particles + aqua-form of vitamin B_{12} (aquacobalamin, H_2OCbl)	-24
BSA particles + nucleotide-free analogue of vitamin B_{12} (ACCby)	-17

SEM study of samples morphology (Fig. 3) confirmed the strong interactions of aquacobalamin and its nucleotide-free analogue with BSA particles.

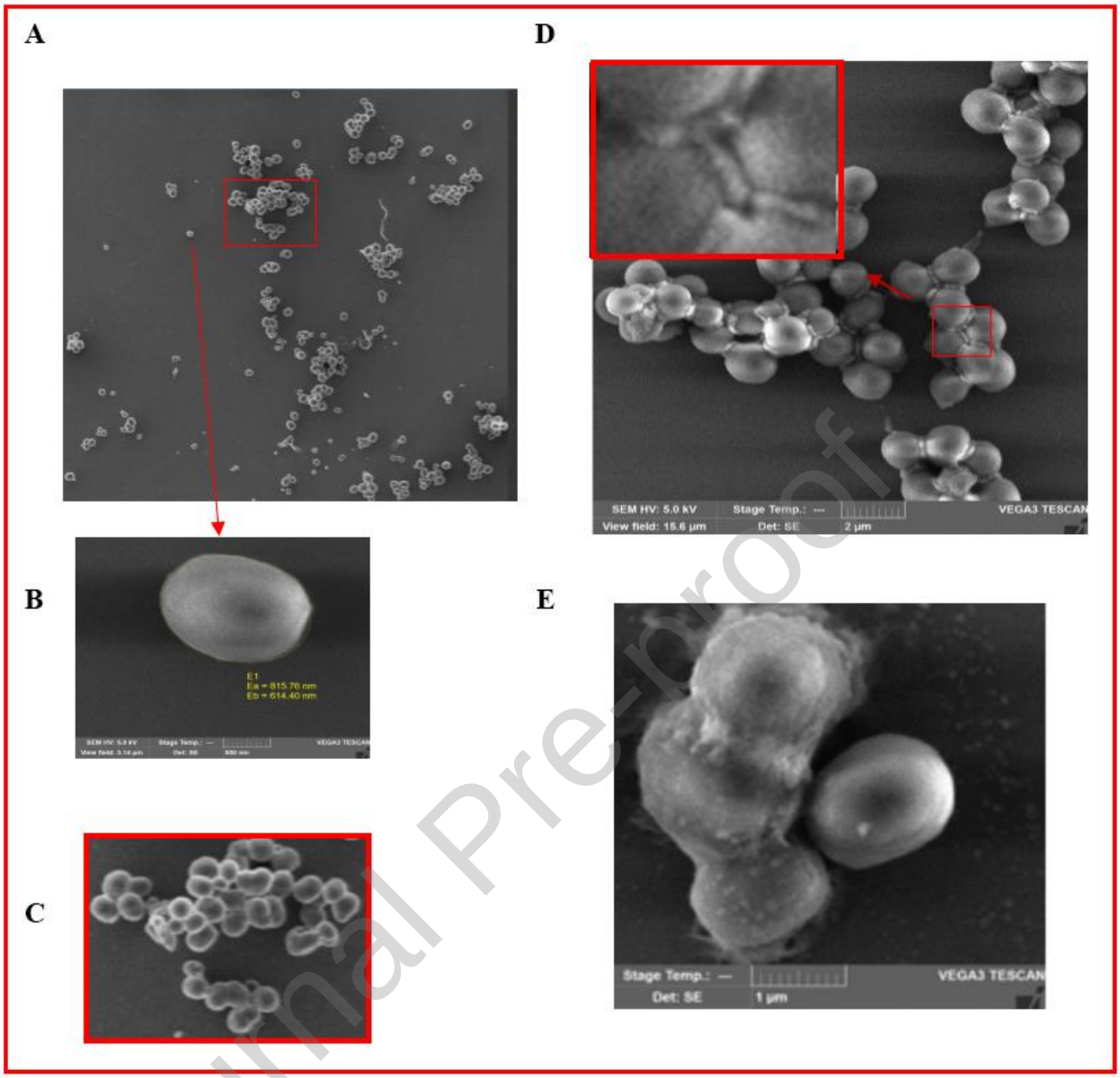

Fig. 3. SEM images of empty BSA particles (A), empty BSA particle (B) and their group (C) on the enlarged scale [red rectangle in (A)]. BSA particles loaded by aqua-form of vitamin B_{12} (D), BSA particles loaded by nucleotide-free analogue of vitamin B_{12} (E).

Comparing images for empty particles (Fig. 3A) and particles loaded with aqua-form of vitamin B_{12} (Fig. 3D) indicates that shape of empty particles is an ellipse (Fig. 3B, 816 nm x 614 nm), the shape of filled ones is close to spherical. Merging of individual particles is not observed. A ‘necklace’ (near 600 nm) consisting of H_2OCbl beads (nano-sized particles of around 100 nm)

surrounds the BSA particles in places of particles contact (Fig. 3D), although they may be formed upon drying containers on the silicon surface.

In the case of nucleotide-free analogue of vitamin B_{12}, high loading of BSA particles is visually observed; in this case, the containers are partially merged (Fig. 3E), which can be explained by the partial unfolding of molecules upon the ACCby binding producing hydrophobic sites on the surface and the strong contact of hydrophobic sites of neighboring molecules. On the surface of containers ACCby particles with a diameter of 30–100 nm (Fig. 3E) can be observed. They may emerge on the surface of the containers upon drying or exist on the surface in solution. Taking into account notable changes in zeta potential (Table 1) of BSA particles after loading with ACCby and H_2OCbl, which reflects changes in their surface properties, their partial merging in solution is likely. This suggestion is supported by the absence of merging of empty BSA particles as well (Fig. 3A).

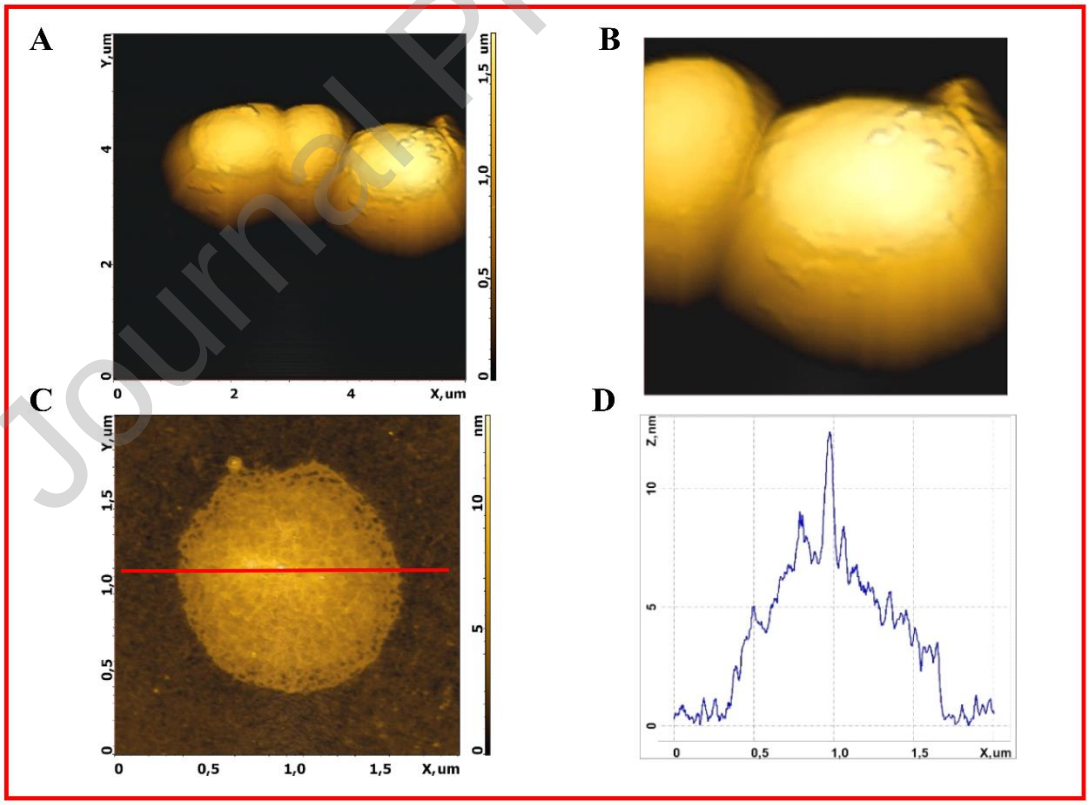

Fig. 4. AFM images of BSA particles loaded by the nucleotide-free analogue of vitamin B_{12}: (A) immediately after applying the solution of BSA particles to the silicon surface, (B) the particles

on an enlarged scale [red rectangle in A], (C) dried BSA particles by the nucleotide-free analogue of vitamin B_{12}, (D) the profile corresponding to the red line in (C).

BSA particles loaded with ACCby were investigated using AFM (Fig. 4). Figs. 4 A and B support merging of two BSA particles loaded with ACCby and the presence of ACCby nanoparticles on the surface of containers. In dried containers (Fig. 4 C), ACCby nanoparticles are well observed. Size of nanoparticles determined using profile indicated in Fig. 4D is 30-100 nm.

Next, we studied incorporation of vitamin B_{12}, its aqua-form, and nucleotide-free analogue using UV-vis spectroscopy. In the case of vitamin B_{12} (CNCbl), UV-vis spectra of species in aqueous solution and in containers are very close (Fig. 5A) indicating absence of strong interaction between CNCbl and BSA particles. UV-vis spectra of aqua-form of vitamin B_{12} (H_2OCbl) in aqueous solution and H_2OCbl incorporated in BSA particles differ significantly (Fig. 5B), i.e., binding with BSA shifts α-band from 526 to 560 nm. The spectrum H_2OCbl bound with BSA particles is characteristic to Co(III)-thiolate species [49,50] (e.g., to the complex of Co(III)-form of Cbl with cysteine, Fig. 3B). Note that the reaction between H_2OCbl and native BSA does not result in the formation of thiolato-complex [44]. The origin of cysteine residue in BSA particles binding H_2OCbl is unclear, i.e., BSA contains only one unoxidized cysteine (Cys43) [51] or cysteine can be generated via the reduction disulfide bonds by sodium borohydride used in the synthesis of BSA particles. However, the complex of H_2OCbl with reduced BSA is unstable [44] that contrasts to stable thiolate complex with BSA particles. In the case of nucleotide-free analogue of vitamin B_{12} (ACCby), the UV-vis spectrum in aqueous solution differs from that of the complex with BSA particles (Fig. 3C). Moreover, for the encapsulated ACCby, the UV-vis spectrum is distinct from that for ACCby-BSA complex (viz. the mixture of amino and imidazole-bound species [45]). However, the UV-vis spectrum of ACCby in BSA carriers is the same as the spectrum of nanoparticles of $AC^{Bu}Cby$, a close homologue of ACCby generated at the air-water interface and transferred onto quartz plates using Langmuir-Schaefer (LS) technique recently

reported by us [35, 52]. Thus, we assume that nanoparticles of nucleotide-free analogue of vitamin B_{12} formed in BSA particles due to self-assembly in confined space at the nanolevel, i.e., the process resembling SMEs formation at the air-water interface.

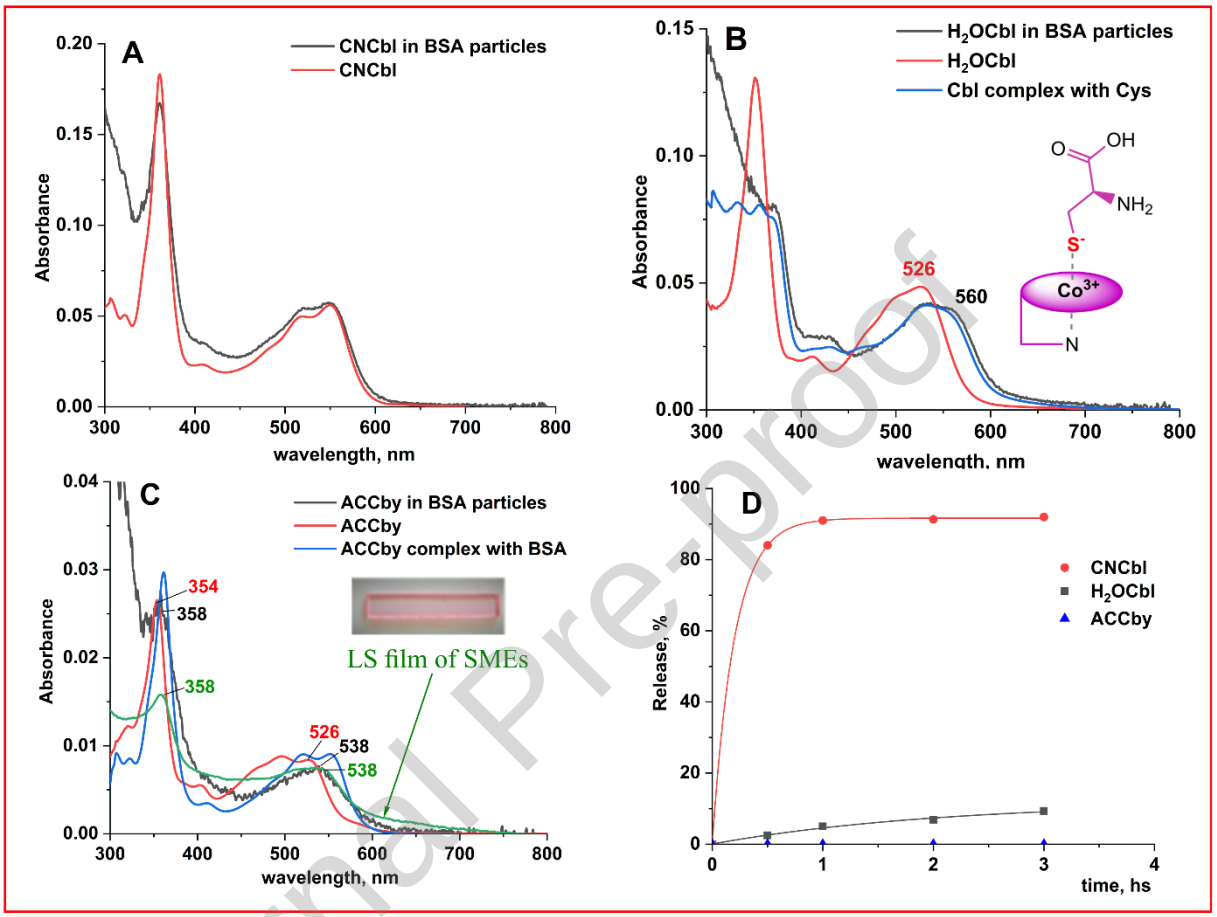

Fig. 5. UV-vis spectra of vitamin B_{12} (CNCbl; A), its aqua-form (H_2OCbl; B), and nucleotide-free analogue (ACCby; C) species relevant to this study. Insets: the complex of H_2OCbl with cysteine (B) and quartz plate covered by LS film of $AC^{Bu}Cby$ SMEs (C). (D) CNCbl, H_2OCbl and ACCby release curves from BSA particles in physiological solution fitted to exponential equation. Fitting gives rate constants of (5.0 ± 0.1) and (0.55 ± 0.20) h^{-1} for CNCbl and H_2OCbl release, respectively.

Using all received data, the following conclusions can be drawn: (i) the mode of binding/incorporation of the studied complexes in BSA particles depends on their structure, i.e., CNCbl weakly interacts with the protein matrix, H_2OCbl produces a strong complex with cysteine residues, and ACCby forms nanoparticles, which is important for their release in vivo and

bioavailability as drugs; (ii) the surface properties of BSA particles might be altered upon incorporation of vitamin B_{12} or its derivatives, which leads to partial merging of containers.

Next, the loading of BSA particles with CNCbl and ACCby was studied using differential scanning calorimetry. Native BSA participates in two independent unfolding events at the thermal midpoints of 56 (a major transition) and 69 °C ([53]; DOI 10.1023/A:1022851809481). In the case of empty BSA particles, the single transition occurs at ca. 64 °C (Fig. S2). Thus, a cross-linking BSA molecules may facilitate its resistance to unfolding. Incorporation of CNCbl to the particles leads to significant decrease in intensity of peak on the DSC curve, whereas ACCby loading notably increases intensity of the DSC peak and shifts it to 73 °C (Fig. S2). This result may be explained by the partial merging of the BSA particles loaded with ACCby observed by SEM (Fig. 3E), i.e., addition of ACCby species facilitates the partial unfolding of BSA particles and produces hydrophobic sites on their surface. Shifting of the DSC peak to higher temperatures upon incorporating ACCby resembles binding of fatty acids by domain III of BSA [53], which may be involved in the hydrophobic interactions with ACCby as was suggested on the basis of spectroscopic data (Fig. 5). Moreover, in the case of BSA particles loaded by ACCby, heating may lead to reduction of Co(III) center to Co(II) species.

We studied release kinetics of vitamin B_{12}, its aqua-form, and nucleotide-free analogue from BSA particles to the saline solution. 83% of CNCbl is released from the containers within 30 minutes; more than 90% of the encapsulated substance is released in 1 hour (Fig. S3A). In the case of H_2OCbl, 16% of the complex is escaped from the BSA particles for 24 hours and no further release occurs (Fig. S3A), which can be explained by high strength of Cbl(III)-S bond [54]. Release of CNCbl and labile fraction of H_2OCbl is described by the first order model (Fig. 5D), and the rate constants of the processes involving CNCbl and H_2OCbl are (5.0 ± 0.1) and (0.55 ± 0.20) h^{-1}, respectively. The half-time of CNCbl and H_2OCbl (a labile fraction) release is (0.14 ± 0.01) and (1.5 ± 0.5) h, respectively. ACCby remains bound with BSA particles under the selected conditions. Thus, SEM data and release experiments indicate that ACCby forms nanoparticles in

the pores of the BSA particle, which are efficiently retained by the protein structure. These nanoparticles themselves do not have specific interactions with BSA. We believe that they are present in the pores of BSA due to their size and hydrophobic interactions. Note that the model conditions used to study the release of complexes differ significantly from in vivo conditions. Further model experiments on the release of H_2OCbl and ACCby included the hydrolysis of the protein matrix of particles by the mixture of proteases (viz. by pronase). Pronase destroys almost all peptide bonds in proteins and peptides [55]. Optical microscopy showed the dissolution of BSA particles within 2 hours as a result of hydrolysis by pronase, leading to the release of encapsulated complexes into the solution. Interestingly that UV-vis spectrum of H_2OCbl after the release is the same as in the particles (Fig. S3B), i.e., it is escaped as thiolate complex.

Prior to examination medicinal properties of BSA particles loaded with vitamin B_{12} and its nucleotide-free analogue, we attempted to determine cytotoxicity of ACCby and its encapsulated version on fibroblast cells (note that cyano- and aquacobalamins are non-toxic). The nucleotide-free analogue of vitamin B_{12} exhibited a noticeable toxic effect at concentrations above 0.35 mM, and the IC50 value was 0.401 mM (Fig. S4A). However, these concentrations cannot be reached for the encapsulated version of the drug. Thus, empty BSA particles and particles loaded with the drug had no significant cytotoxic activity against fibroblasts (Fig. S4B).

We analyzed the ability of free and encapsulated ACCby to stimulate the formation of necrotic and apoptotic populations after 48 and 72 h of incubation (Fig. S4). Necrotic populations were almost completely absent in all samples, which is most likely due to the incubation method and cell samples treatment - cells were adhered on culture plates during incubation and washed before staining, which allowed to detach poorly adhered late apoptotic or necrotic cells. However, the observed apoptotic populations allowed us to compare the toxicity of the samples.

In control samples, the formation of apoptotic cell populations was observed after 48 and 72 hours at a level of 5-8% (Fig. S5). After 48 hours of incubation with empty BSA particles, about 14% of cells were observed in the apoptotic stage and 17-18% after 72 hours. A similar

picture was observed for BSA particles containing ACCby: after 48 hours, the value of apoptotic populations was 10-12%, and after 72 hours – 16-17%. With respect to the ACCby, the cells showed a more sensitive phenotype, especially after 72 hours of incubation: after 48 hours, the value of apoptotic populations was 14-17%, and after 72 hours – 34-40%. Note that no obvious dose-dependent effect was observed for all studied samples. The obtained data indicate that the inclusion of the ACCby in the BSA particles likely reduces the toxic effect of the compound on cells. Furthermore, we observed no obvious differences between treated by free and encapsulated ACCby and control cells during microscopy (Fig. S6).

For further experiments involving animals, an encapsulated form of nucleotide-free vitamin B_{12} analogue was introduced in concentrations (30 μg/ml) that are within the range utilized for assessing cytotoxicity (i.e., in non-toxic doses).

3.2. The effects of CNCbl, H_2OCbl and ACCby encapsulated in BSA particles on a model of primary generalized seizures in rats

Next, the study was performed using four groups of rats. In all groups, BSA particles (i.e., empty BSA particles and particles loaded by CNCbl, H_2OCbl and ACCby) were preventively administered to the animals for 18 days animals. After the administration of BSA particles, a single injection of thiosemicarbazide was carried out. In the control group (n=6), empty BSA particles were introduced, BSA particles containing CNCbl, H_2OCbl and ACCby were introduced in the other groups (n=6 for each group).

In animals of the control group, when thiosemicarbazide was administered at the indicated dose, primary generalized convulsions were observed in 100% of cases in the form of flinching, manege running, clonic convulsions, tonic-clonic convulsions with a lateral position, and tonic extension. Mortality in this group was 100%.

Administration of CNCbl loaded in BSA particles did not significantly reduce the severity and intensity of convulsive attacks compared to the control group (Table S1), but mortality decreased (67%). In the group of animals that received particles loaded with aquacobalamin, duration, nature and severity of seizures were the same as those in the second (received CNCbl) and fourth (received ACCby) groups of animals, no significant differences were observed. However, mortality was reduced (67%) in the group of rats that were administered BSA particles with ACCby.

In all observations of the control group after the reproduction of primary generalized seizures, the studied parts of the brain had significant circulatory disorders, characterized by stasis of erythrocytes in the capillaries, the formation of fibrin-erythrocyte thrombi in the lumens of small veins of the gray and white matter of the brain, paresis and congestion of the veins with the development of pronounced perivascular swelling of the nervous tissue (Fig. 6A). In the pial and intracerebral arteries, changes in the contours of the elastic intimal membrane were noted against the background of narrowing of the lumen of the vessels, which characterizes persistent spasm of the arterial link (Fig. 6B). In conditions of impaired vascular permeability, in 4 of 6 cases in the control group, hemorrhagic impregnation of the pia mater of the cerebrum was detected.

Pathohistological examination of the gray matter of the cerebral hemispheres and cerebellum revealed the predominance of ischemic type of neuronal damage. In many fields of view, entire groups of pycnomorphic and hyperchromic neurons with signs of neurophagia were found with an increase in the activity of microglial elements in the damaged areas (Fig. 6C). At the same time, some neurons were characterized by acute swelling with vacuolization of the cytoplasm, focal or diffuse chromatolysis (Fig. 6D).

In the group of rats, which received a solution containing encapsulated CNCbl, circulatory disorders in microvasculature were characterized by diffuse focal hemostasis in the capillaries, congestion of the intracerebral and pial veins, moderate pericapillary edema of the nervous tissue of the cortex and white matter of the cerebral hemispheres and brain stem (Fig. 6E). The lumen of

the extracerebral arteries of the muscular type was slightly narrowed due to contraction of the muscle layer (Fig. 6F).

Analysis of structural changes in neurocytes showed a decrease in the number of irreversibly damaged cells of the ischemic type (Fig. 6G), structural changes in nerve cells were largely reversible (in the form of focal fusion of Nissl lumps, formation of vacuoles in the cytoplasm, moderate swelling of the nucleus and axonal process, see Fig. 6H). In all observations, separate zones, where neurocytes remained intact, were identified.

With the introduction of BSA particles loaded with H_2OCbl, circulatory disorders in the brain of animals were characterized by moderately pronounced spasm of small-caliber arteries, hemostasis in the vessels of the central nervous system and perivascular edema of the nervous tissue (Fig. 6I); in the second and fifth observations, single small-focal hemorrhages in the nervous tissue were found (Fig. 6J). Neuronal damage took the form of both local irreversible and widespread reversible changes. Among the irreversible changes, the ischemic variant predominated. In single pyramidal neurons and Purkinje cells, hyperchromia and homogenization of the cytoplasm, karyopyknosis were observed, pyramidal neurons lost their usual geometric shape, piriform neurons had swollen, tortuous axons (Fig. 6K). Along with ischemic damage, individual neurocytes showed signs of acute swelling with the disappearance of Nissl lumps. Reversible changes in nerve cells were noted; they prevailed over deep damage, which was characterized by swelling and deformation of the nuclei, diffuse small-focal chromatolysis of the cytoplasm (Fig. 6L).

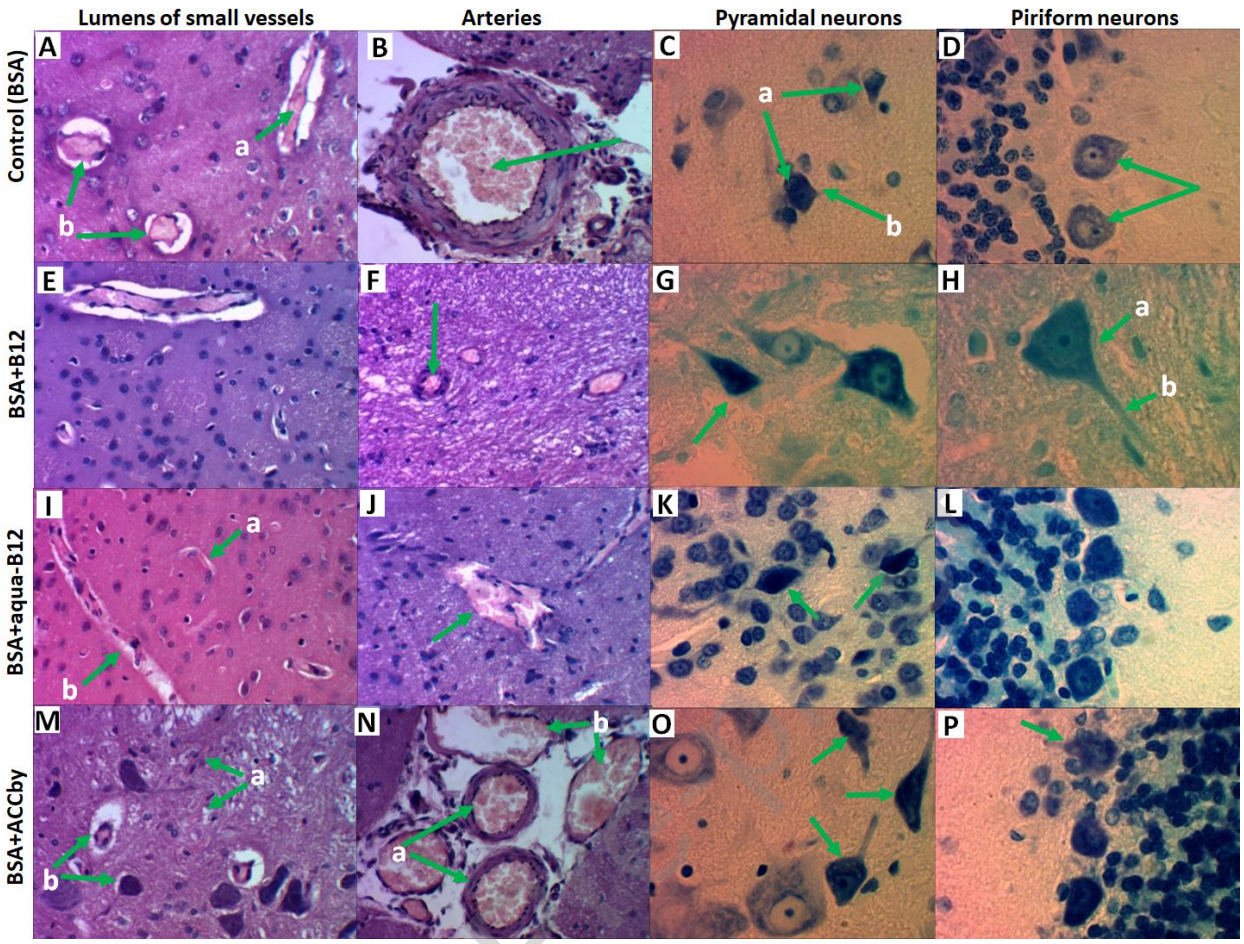

Fig. 6. Histological analysis of brain tissue using nanoencapsulated vitamin B_{12} derivatives in the thiosemicarbazide model of seizures. Hematoxylin and eosin staining, magnification x480 (slides A, B, E, F, I, J, M, N). Staining with toluidine blue according to Nissl, magnification x1200 (slides C, D, G, H, K, L, O, P). A) Fibrin-erythrocyte thrombi in the lumens of capillaries and venules ("a"), congestion of the veins, perivascular edema of the nervous tissue of the forebrain cortex ("b"). (B) Spastic condition of the pial artery. (C) Pyknotic hyperchromatic pyramidal neurons ("a"), proliferation of microglia, beginning of the formation of a neurophagic nodule ("b"). (D) Focal hydrolysis, vacuolization of the cytoplasm of piriform neurons of the cerebellum. (E) Stasis of erythrocytes in the lumens of capillaries and venules, moderate perivascular edema of the nervous tissue of the cerebral hemispheres. (F) Moderate spasm of the intracerebral artery. (G) Focal irreversible damage to the forebrain pyramidal neuron. (H) Homogenization of the cytoplasm, moderate swelling of the brainstem neuron nucleus ("a"), axonal edema ("b"). (I) Stasis of erythrocytes in the capillaries ("a"), congestion of the venule, perivenular edema of the nervous

tissue (“b”). (J) Small focal diapedetic hemorrhage in the cerebral cortex. (K) Hyperchromic pycnomorphic pyramidal neurons against the background of microglial proliferation. (L) Reversible changes in piriform neurons with diffuse small focal chromatolysis. (M) Stasis of erythrocytes in capillaries (“a”), pronounced perivascular and pericellular edema of the nervous tissue of the brain stem (“b”). (N) Moderate spasm of the pial arteries (“a”), paresis and congestion of the pia mater veins (“b”). (O) A group of hyperchromic, pycnomorphic pyramidal neurons with deformation and swelling of axons. (P) Death of a piriform neuron with a perifocal reaction of neuroglia (the so-called neurophagic nodule).

When BSA particles with ACCby were administered, more pronounced circulatory disorders were noted in the form of diffuse focal hemostasis in capillaries and venules, perivascular and pericellular edema of the nervous tissue (Fig. 6M). Spasm of the pial and intracerebral arteries persisted, the severity of which was comparable to changes in group 4 (control) (Fig. 6N). Damage to neurons in the cerebral hemispheres and cerebellum was diffuse-focal in nature with a predominance of ischemic changes in the form of hyperchromia and a decrease in the volume of cytoplasm while maintaining the nuclei (Fig. 6O); the death of individual neurons was accompanied by an active reaction of microglia with the formation of neurophagic nodules (Fig. 6P). Morphometric analysis of structural changes in neurons confirmed a slight decrease in irreversible changes in neurons in all groups receiving BSA particles with CNCbl, H_2OCbl and ACCby (Table S2).

Therefore, we assume that release of vitamin B_{12} and its derivatives from BSA particles may proceed via two routes, i.e., (i) a direct dissociation of CNCbl from the particles, and (ii) a preliminary proteolysis in the blood or tissues of the particles and further liberation of ACCby. Next, transcobalamin II binds CNCbl and transports it inside cells. Further intracellular processing converts CNCbl into cofactor forms [56]. The activity of methylmalonyl-CoA mutase utilizing adenosylcobalamin as a cofactor is important for neuroprotection, i.e., this enzyme is involved in

the conversion of toxic methylmalonic acid to succinic acid [1]. Note that methylmalonic acid possesses neurotoxicity and can induce oxidative stress [57]. The in vivo action of ACCby does not depend on cobalamin-dependent proteins [58,59] and its action may be mediated by unspecific reactions with biomolecules. In the case of BSA particles loaded with H_2OCbl, their proteolysis leads to formation of H_2OCbl complex with unhydrolyzed part of protein, which, apparently, cannot be utilized by cobalamin-dependent proteins. This fact explains absence of neuroprotective effect of BSA particles loaded with H_2OCbl.

Thiosemicarbazide causes reversible seizures by modulating GABAergic processes via inhibiting glutamic acid decarboxylase [60]. Cobalamins and their nucleotide-free analogue do not react directly with thiosemicarbazide [43]. However, administration of thiosemicarbazide derivatives can cause oxidative stress [61]. Cobalamins and their derivatives possess pronounced antioxidant properties [10,62]. Thus, we hypothesize that corrinoid-assisted detoxication of thiosemicarbazide may be caused by their ability to ameliorate oxidative stress. Note that CNCbl can exhibit simultaneously functions as an antioxidant [62] and the precursor of the methylmalonyl-CoA mutase cofactor [1], which detoxifies methylmalonic acid.

4. Conclusion

Here, we showed that vitamin B_{12} (cyano- and aquacobalamins) and their nucleotide-free analogue can be successfully encapsulated in BSA particles. Cyanocobalamin is weakly retained by BSA particles and relatively freely escapes to the solution, whereas aquacobalamin strongly binds with thiol groups of the particles, and its release to the solution requires proteolytic destruction of the carriers. Notably both from a fundamental and applied point of view, that heptamethyl ester of aquacyanocobyrinic acid (ACCby), a weakly water-soluble derivative of vitamin B_{12}, is present in the BSA containers in the form of nanoparticles resembling those generated by its close homologue (viz. heptabutyl cobyrinate) due to self-assembly in confined space at the nanolevel at the air-water interface [35]. This own nanoform of the drug allows it to

avoid strong interaction with the BSA matrix and reach therapeutic effects comparable to those of free ACCby.

Using the model of primary generalized seizures in rats induced by the pharmacotoxicant thiosemicarbazide, we showed that administration of BSA carriers with cyanocobalamin and ACCby exhibit a neuroprotective effect. The best influence of the encapsulation on the effectiveness of the drug was achieved in the case of ACCby, whose bioavailability as a neuroprotector did not change upon introduction in BSA particles, i.e., 33% of surviving animals were observed upon ACCby administration in free form and in encapsulated state. No surviving rats were observed without the administration of drugs. Probably, BSA particles undergo partial or complete proteolytic destruction in tissues or blood, which leads to release of drugs. Regarding the mechanism of neutralizing thiosemicarbazide toxic effects, we hypothesize that it may proceed via scavenging of reactive oxygen or other species produced upon thiosemicarbazide metabolism by vitamin B_{12} or its derivatives, whereas CNCbl, in addition to the former, acts as the precursor of the methylmalonyl-CoA mutase cofactor, which detoxifies methylmalonic acid.

The results indicate that BSA particles loaded with vitamin B_{12} derivatives may represent a medicinal interest. In particular, targeted delivery of vitamin B_{12} derivatives utilizing BSA-based carriers is of special interest. For example, the carriers may be loaded with forms of vitamin B_{12} containing fluorescent or radioactive labels for visualizing required cells [63,64], antivitamins acting as inhibitors of cobalamin-dependent processes, donors of cytotoxic species [65], or their combinations for nanotheranostics purposes (e.g., for simultaneous imaging and destruction of cells). Modification of BSA particles for efficient targeted delivery of cytotoxic vitamin B_{12} derivatives, in particular, to specific tumor cells represents interest for additional research. Further studies can be aimed at determining the kinetic parameters and mechanisms of vitamin B_{12} and its derivatives release from BSA particles under in vivo conditions (including assessing the stability of BSA particles in blood and tissues, inflammatory stimulation, immune activation, protein expression etc.), which can be achieved via labeling their structures (e.g., using fluorescent labels).

Moreover, the mechanisms of the in vivo action of vitamin B_{12} semi-synthetic derivatives are poorly understood, and additional work is required to elucidate them.

Acknowledgments

This work was supported by the grant of the Russian Science Foundation (20-12-00175-p), Ivanovo State University of Chemistry and Technology (ISUCT), and Ministry of Science and Higher Education of the Russian Federation (MSHE of RF) (FZZW-2023-0009, AFM study). The authors acknowledge the MSHE of RF for the resources provided by the Centers for Shared Use of Scientific Equipment of the ISUCT, Ivanovo (project 075-15-2021-671) and of Center "Structural diagnostics of materials" within the framework of the state assignment of Kurchatov Complex Crystallography and photonics, NRC "Kurchatov Institute" (customizing the spectrophotometer for research tasks).

Declaration of competing interest

The authors declare that they have no known competing financial interests or personal relationships that could have appeared to influence the work reported in this paper.

Data availability

Data will be made available on request.

Appendix A. Supplementary data

Supplementary material related to this article can be found, in the online version, at doi:

References

[1] B. Kräutler, Vitamin B_{12}: chemistry and biochemistry, Biochem. Soc. Trans. 33 (2005) 806–810. https://doi.org/10.1042/BST0330806.

[2] S.W. Borron, F.J. Baud, B. Mégarbane, C. Bismuth, Hydroxocobalamin for severe acute cyanide poisoning by ingestion or inhalation, Am. J. Emerg. Med. 25 (2007) 551–558. https://doi.org/10.1016/j.ajem.2006.10.010.

[3] A. Chan, J. Jiang, A. Fridman, L.T. Guo, G.D. Shelton, M.-T. Liu, C. Green, K.J. Haushalter, H.H. Patel, J. Lee, D. Yoon, T. Burney, D. Mukai, S.B. Mahon, M. Brenner, R.B. Pilz, G.R. Boss, Nitrocobinamide, a New Cyanide Antidote That Can Be Administered by Intramuscular Injection, J. Med. Chem. 58 (2015) 1750–1759. https://doi.org/10.1021/jm501565k.

[4] P.C. Ng, T.B. Hendry-Hofer, N. Garrett, M. Brenner, S.B. Mahon, J.K. Maddry, P. Haouzi, G.R. Boss, T.F. Gibbons, A.A. Araña, V.S. Bebarta, Intramuscular cobinamide versus saline for treatment of severe hydrogen sulfide toxicity in swine, Clin. Toxicol. 57 (2019) 189–196. https://doi.org/10.1080/15563650.2018.1504955.

[5] T.B. Hendry-Hofer, P.C. Ng, A.M. McGrath, K. Soules, D.S. Mukai, A. Chan, J.K. Maddry, C.W. White, J. Lee, S.B. Mahon, M. Brenner, G.R. Boss, V.S. Bebarta, Intramuscular cobinamide as an antidote to methyl mercaptan poisoning, Inhal. Toxicol. 33 (2021) 25–32. https://doi.org/10.1080/08958378.2020.1866123.

[6] G.K. Schwaerzer, H. Kalyanaraman, D.E. Casteel, N.D. Dalton, Y. Gu, S. Lee, S. Zhuang, N. Wahwah, J.M. Schilling, H.H. Patel, Q. Zhang, A. Makino, D.M. Milewicz, K.L. Peterson, G.R. Boss, R.B. Pilz, Aortic pathology from protein kinase G activation is prevented by an antioxidant vitamin B12 analog, Nat. Commun. 10 (2019) 3533. https://doi.org/10.1038/s41467-019-11389-1.

[7] F. Zelder, Recent trends in the development of vitamin B_{12} derivatives for medicinal applications, Chem. Commun. 51 (2015) 14004–14017. https://doi.org/10.1039/C5CC04843E.

[8] A. Chan, M. Balasubramanian, W. Blackledge, O.M. Mohammad, L. Alvarez, G.R. Boss, T.D. Bigby, Cobinamide is superior to other treatments in a mouse model of cyanide poisoning, Clin. Toxicol. 48 (2010) 709–717. https://doi.org/10.3109/15563650.2010.505197.

[9] M. Brenner, S. Benavides, S.B. Mahon, J. Lee, D. Yoon, D. Mukai, M. Viseroi, A. Chan, J. Jiang, N. Narula, S.M. Azer, C. Alexander, G.R. Boss, The vitamin B12 analog cobinamide is an effective hydrogen sulfide antidote in a lethal rabbit model, Clin. Toxicol. 52 (2014) 490–497. https://doi.org/10.3109/15563650.2014.904045.

[10] S. Chang, J. Tat, S.P. China, H. Kalyanaraman, S. Zhuang, A. Chan, C. Lai, Z. Radic, E.A. Abdel-Rahman, D.E. Casteel, R.B. Pilz, S.S. Ali, G.R. Boss, Cobinamide is a strong and versatile antioxidant that overcomes oxidative stress in cells, flies, and diabetic mice, PNAS Nexus 1 (2022) pgac191. https://doi.org/10.1093/pnasnexus/pgac191.

[11] L.A. Maiorova, S.I. Erokhina, M. Pisani, G. Barucca, M. Marcaccio, O.I. Koifman, D.S. Salnikov, O.A. Gromova, P. Astolfi, V. Ricci, V. Erokhin, Encapsulation of vitamin B_{12} into nanoengineered capsules and soft matter nanosystems for targeted delivery, Colloids Surf. B Biointerfaces 182 (2019) 110366. https://doi.org/10.1016/j.colsurfb.2019.110366.

[12] T.T. Vu, L.A. Maiorova, D.B. Berezin, O.I. Koifman, Formation and Study of Nanostructured M-Monolayers and LS-Films of Triphenylcorrole, Macroheterocycles 9 (2016) 73–79. https://doi.org/10.6060/mhc151205m.

[13] L.A. Maiorova, N. Kobayashi, S.V. Zyablov, V.A. Bykov, S.I. Nesterov, A.V. Kozlov, C.H. Devillers, A.V. Zavyalov, V.V. Alexandriysky, M. Orena, O.I. Koifman, Magnesium Porphine Supermolecules and Two-Dimensional Nanoaggregates Formed Using the Langmuir–Schaefer Technique, Langmuir 34 (2018) 9322–9329. https://doi.org/10.1021/acs.langmuir.8b00905

[14] L.A. Valkova, L.S. Shabyshev, N.Yu. Borovkov, L.A. Feigin, F. Rustichelli, Supramolecular Assembly Formation in Monolayers of tert-Butyl Substituted Copper Phthalocyanine and Tetrabenzotriazaporphin, J. Incl. Phenom. Macrocycl. Chem. 35 (1999) 243–249. https://doi.org/10.1023/A:1008147031935.

[15] L.A. Valkova, L.S. Shabyshev, L.A. Feigin, O.B. Akopova, Formation and X-ray diffraction investigation of Langmuir-Blodgett films of liquid crystalline substituted crown esters, Mol. Cryst. Liq. Cryst. Sci. Technol. 6 (1996) 291–298.

[16] S. Soares, J. Sousa, A. Pais, C. Vitorino, Nanomedicine: Principles, Properties, and Regulatory Issues, Front. Chem. 6 (2018) 360. https://doi.org/10.3389/fchem.2018.00360.

[17] M. Nowak, T.D. Brown, A. Graham, M.E. Helgeson, S. Mitragotri, Size, shape, and flexibility influence nanoparticle transport across brain endothelium under flow, Bioeng. Transl. Med. 5 (2020) e10153. https://doi.org/10.1002/btm2.10153.

[18] A. Zeytunluoglu, I. Arslan, Current Perspectives on Nanoemulsions in Targeted Drug Delivery, in: Handbook of Research on Nanoemulsion Applications in Agriculture, Food, Health, and Biomedical Sciences, 2022: pp. 118–140. https://doi.org/10.4018/978-1-7998-8378-4.ch006.

[19] M. Du, Y. Ouyang, F. Meng, X. Zhang, Q. Ma, Y. Zhuang, H. Liu, M. Pang, T. Cai, Y. Cai, Polymer-lipid hybrid nanoparticles: A novel drug delivery system for enhancing the activity of Psoralen against breast cancer, Int. J. Pharm. 561 (2019) 274–282. https://doi.org/10.1016/j.ijpharm.2019.03.006.

[20] D. de Moraes Profirio, F.B.T. Pessine, Formulation of functionalized PLGA nanoparticles with folic acid-conjugated chitosan for carboplatin encapsulation, Eur. Polym. J. 108 (2018) 311–321. https://doi.org/10.1016/j.eurpolymj.2018.09.011.

[21] K. Ariga, M. Nishikawa, T. Mori, J. Takeya, L.K. Shrestha, J.P. Hill, Self-assembly as a key player for materials nanoarchitectonics, Sci. Technol. Adv. Mater. 20 (2019) 51–95. https://doi.org/10.1080/14686996.2018.1553108.

[22] W.A. Webre, H.B. Gobeze, S. Shao, P.A. Karr, K. Ariga, J.P. Hill, F. D'Souza, Fluoride-ion binding promoted photoinduced charge separation in a self-assembled C60 alkyl cation bound bis-crown ether-oxoporphyrinogen supramolecule, Chem. Commun. 54 (2018) 1351–1354. https://doi.org/10.1039/C7CC09524D.

[23] I.N. Topchieva, S. V. Osipova, M.I. Banatskaya, L.A. Valkova, Membrane-active properties of block-copolymers of ethylene-oxide and propylene-oxide, Dokl. Akad. Nauk SSSR 308 (1989) 910–913.

[24] L.A. Valkova, A.S. Glibin, L. Valli, Quantitative analysis of compression isotherms of fullerene C60 Langmuir layers, Colloid J. 70 (2008) 6–11. https://doi.org/10.1134/S1061933X0801002X

[25] A.N. Oldacre, A.E. Friedman, T.R. Cook, A self-assembled cofacial cobalt porphyrin prism for oxygen reduction catalysis, J. Am. Chem. Soc. 139 (2017) 1424−1427. https://doi.org/10.1021/jacs.6b12404.

[26] W. Brenner, T.K. Ronson, J.R. Nitschke, Separation and selective formation of fullerene adducts within an MII 8L6 cage, J. Am. Chem. Soc. 139 (2017) 75–78. https://doi.org/10.1021/jacs.6b11523.

[27] K. Ariga, T. Mori, W. Nakanishi, J.P. Hill, Solid surface vs. liquid surface: nanoarchitectonics, molecular machines, and DNA origami, Phys. Chem. Chem. Phys. 19 (2017) 23658–23676. https://doi.org/10.1039/C7CP02280H.

[28] K. Ariga, K.C. Tsai, L.K. Shrestha, S.H. Hsu, Life science nanoarchitectonics at interfaces, Mater. Chem. Front. 5 (2021) 1018–1032. https://doi.org/10.1039/D0QM00615G.

[29] N.K. Shee, M.K. Kim, H.J. Kim, Supramolecular Porphyrin Nanostructures Based on Coordination-Driven Self-Assembly and Their Visible Light Catalytic Degradation of Methylene Blue Dye, Nanomaterials 10 (2020) 2314–2329. https://doi.org/10.3390/nano10112314.

[30] E. Stulz, Nanoarchitectonics with porphyrin functionalized DNA, Acc. Chem. Res. 50 (2017) 823−831. https://doi.org/10.1021/acs.accounts.6b00583.

[31] L. Valkova, A. Menelle, N. Borovkov, V. Erokhin, M. Pisani, F. Ciuchi, F. Carsughi, F. Spinozzi, M. Pergolini, R. Padke, S. Bernstorff, F. Rustichelli, Small-angle X-ray scattering and neutron reflectivity studies of Langmuir–Blodgett films of copper tetra-*tert* -butyl-azaporphyrines, J. Appl. Crystallogr. 36 (2003) 758–762. https://doi.org/10.1107/S0021889803004965.

[32] L. Valkova, C. Betrencourt, A. Hochapfel, I. V. Myagkov, L.A. Feigin, Monolayer Study of Monensin and Lasalocid in the Gas State, Mol. Cryst. Liq. Cryst. Sci. Technol. A Mol. Cryst. Liq. Cryst. 287 (1996) 269–273. https://doi.org/10.1080/10587259608038763.

[33] M. V. Karlyuk, Yu.Yu. Krygin, L.A. Maiorova, T.A. Ageeva, O.I. Koifman, Formation of two-dimensional (M) and three-dimensional (V) nanoaggregates of substituted cobalt porphyrin in the Langmuir layers and Langmuir-Schaefer films, Russ. Chem. Bull. 62 (2013) 471–479. https://doi.org/10.1007/s11172-013-0066-5.

[34] N.V. Kharitonova, L.A. Maiorova, O.I. Koifman, Aggregation behavior of unsubstituted magnesium porphyrazine in monolayers at air–water interface and in Langmuir–Schaefer films, J. Porphyrins Phthalocyanines 22 (2018) 509–520. https://doi.org/10.1142/S1088424618500505.

[35] L.A. Maiorova, N. Kobayashi, D.S. Salnikov, S.M. Kuzmin, T. V. Basova, O.I. Koifman, V.I. Parfenyuk, V.A. Bykov, Y.A. Bobrov, P. Yang, Supermolecular Nanoentities of Vitamin B_{12} Derivative as a Link in the Evolution of the Parent Molecules During Self-Assembly at the Air–Water Interface, Langmuir 39 (2023) 3246–3254. https://doi.org/10.1021/acs.langmuir.2c02964.

[36] F. Kratz, Albumin as a drug carrier: Design of prodrugs, drug conjugates and nanoparticles, J. Control. Release 132 (2008) 171–183. https://doi.org/10.1016/j.jconrel.2008.05.010.

[37] W.C. Mak, R. Georgieva, R. Renneberg, H. Bäumler, Protein Particles Formed by Protein Activation and Spontaneous Self-Assembly, Adv. Funct. Mater. 20 (2010) 4139–4144. https://doi.org/10.1002/adfm.201001205.

[38] F. Galisteo-González, J.A. Molina-Bolívar, Systematic study on the preparation of BSA nanoparticles, Colloids Surf. B Biointerfaces 123 (2014) 286–292. https://doi.org/10.1016/j.colsurfb.2014.09.028.

[39] S. Naveenraj, S. Anandan, Binding of serum albumins with bioactive substances – Nanoparticles to drugs, J. Photochem. Photobiol. C Photochem. Rev. 14 (2013) 53–71. https://doi.org/10.1016/j.jphotochemrev.2012.09.001.

[40] A. Parodi, J. Miao, S.M. Soond, M. Rudzińska, A.A. Zamyatnin, Albumin Nanovectors in Cancer Therapy and Imaging, Biomolecules 9 (2019) 218. https://doi.org/10.3390/biom9060218.

[41] G. V. Patil, Biopolymer albumin for diagnosis and in drug delivery, Drug Dev. Res. 58 (2003) 219–247. https://doi.org/10.1002/ddr.10157.

[42] O.A. Gromova, I.Yu. Torshin, L.A. Maiorova, O.I. Koifman, D.S. Salnikov, Bioinformatic and chemoneurocytological analysis of the pharmacological properties of vitamin B_{12} and some of its derivatives, J. Porphyr. Phthalocyanines 25 (2021) 835–842. https://doi.org/10.1142/S1088424621500644.

[43] O.A. Gromova, L.A. Maiorova, D.S. Salnikov, V.I. Demidov, A.G. Kalacheva, I.Yu. Torshin, T.E. Bogacheva, A.N. Gromov, O.A. Limanova, T.R. Grishina, S.M. Jafari, O.I. Koifman, Vitamin B12 Hydrophobic Derivative Exhibits Bioactivity: Biomedical and Photophysical Study, Bionanoscience 12 (2022) 74–82. https://doi.org/10.1007/s12668-021-00916-4.

[44] I.A. Dereven'kov, L. Hannibal, S. V. Makarov, A.S. Makarova, P.A. Molodtsov, O.I. Koifman, Characterization of the complex between native and reduced bovine serum albumin with aquacobalamin and evidence of dual tetrapyrrole binding, J. Biol. Inorg. Chem. 23 (2018) 725–738. https://doi.org/10.1007/s00775-018-1562-8.

[45] I.A. Dereven'kov, I.I. Dzvinkas, V.S. Osokin, S. V. Makarov, Effect of bovine serum albumin on the water solubility of hydrophobic corrinoids, J. Porphyr. Phthalocyanines 27 (2023) 811–817. https://doi.org/10.1142/S1088424623500633.

[46] I.A. Dereven'kov, S. V. Makarov, P.A. Molodtsov, Effect of bovine serum albumin on redox and ligand exchange reactions involving aquacobalamin, Macroheterocycles 13 (2020) 223–228. https://doi.org/10.6060/mhc200498d.

[47] I.A. Dereven'kov, V.S. Osokin, P.A. Molodtsov, A.S. Makarova, S. V. Makarov, Effect of complexation between cobinamides and bovine serum albumin on their reactivity toward cyanide, React. Kinet. Mech. Catal. 135 (2022) 1469–1483. https://doi.org/10.1007/s11144-022-02216-8.

[48] A. Salis, M. Boström, L. Medda, F. Cugia, B. Barse, D.F. Parsons, B.W. Ninham, M. Monduzzi, Measurements and Theoretical Interpretation of Points of Zero Charge/Potential of BSA Protein, Langmuir 27 (2011) 11597–11604. https://doi.org/10.1021/la2024605.

[49] K.S. Conrad, T.C. Brunold, Spectroscopic and Computational Studies of Glutathionylcobalamin: Nature of Co–S Bonding and Comparison to Co–C Bonding in Coenzyme B_{12}, Inorg. Chem. 50 (2011) 8755–8766. https://doi.org/10.1021/ic200428r.

[50] A.S. Eisenberg, I. V. Likhtina, V.S. Znamenskiy, R.L. Birke, Electronic Spectroscopy and Computational Studies of Glutathionylco(III)balamin, J. Phys. Chem. A 116 (2012) 6851–6869. https://doi.org/10.1021/jp301294x.

[51] A. Bujacz, Structures of bovine, equine and leporine serum albumin, Acta Crystallogr. D Biol. Crystallogr. 68 (2012) 1278–1289. https://doi.org/10.1107/S0907444912027047.

[52] I.A. Dereven'kov, L.A. Maiorova, O.I. Koifman, D.S. Salnikov, High Reactivity of Supermolecular Nanoentities of a Vitamin B $_{12}$ Derivative in Langmuir–Schaefer Films Toward Gaseous Toxins, Langmuir 39 (2023) 17240–17250. https://doi.org/10.1021/acs.langmuir.3c02317.

[53] A. Michnik, Thermal stability of bovine serum albumin DSC study, J. Therm. Anal. Calorim. 71 (2003) 509–519. https://doi.org/10.1023/A:1022851809481.

[54] L. Xia, A.G. Cregan, L.A. Berben, N.E. Brasch, Studies on the Formation of Glutathionylcobalamin: Any Free Intracellular Aquacobalamin Is Likely to Be Rapidly and Irreversibly Converted to Glutathionylcobalamin, Inorg. Chem. 43 (2004) 6848–6857. https://doi.org/10.1021/ic040022c.

[55] T.N. Borodina, D.A. Shepelenko, D.B. Trushina, V. V. Artemov, T. V. Bukreeva, Enzymatic Degradation of Capsules Based on Polyelectrolyte Polypeptide–Polysaccharide Complex for the Controlled Release of DNA, Polymer Sci. B 63 (2021) 514–520. https://doi.org/10.1134/S156009042105002X.

[56] R. Banerjee, B_{12} Trafficking in Mammals: A Case for Coenzyme Escort Service, ACS Chem. Biol. 1 (2006) 149–159. https://doi.org/10.1021/cb6001174.

[57] C.G. Fernandes, C.G. Borges, B. Seminotti, A.U. Amaral, L.A. Knebel, P. Eichler, A.B. de Oliveira, G. Leipnitz, M. Wajneret, Experimental Evidence that Methylmalonic Acid Provokes Oxidative Damage and Compromises Antioxidant Defenses in Nerve Terminal and Striatum of Young Rats, Cell. Mol. Neurobiol. 31 (2011) 775–785. https://doi.org/10.1007/s10571-011-9675-4.

[58] E. Stupperich, E. Nexø, Effect of the cobalt-N coordination on the cobamide recognition by the human vitamin B_{12} binding proteins intrinsic factor, transcobalamin and haptocorrin, Eur. J. Biochem. 199 (1991) 299–303. https://doi.org/10.1111/j.1432-1033.1991.tb16124.x.

[59] O.M. Sokolovskaya, T. Plessl, H. Bailey, S. Mackinnon, M.R. Baumgartner, W.W. Yue, D.S. Froese, M.E. Taga, Naturally occurring cobalamin (B_{12}) analogs can function as cofactors for human methylmalonyl-CoA mutase, Biochimie 183 (2021) 35–43. https://doi.org/10.1016/j.biochi.2020.06.014.

[60] R.W. Horton, GABA and seizures induced by inhibitors of glutamic acid decarboxylase, Brain Res. Bull. 5 (1980) 605–608. https://doi.org/10.1016/0361-9230(80)90099-4.

[61] K. Malarz, A. Mrozek-Wilczkiewicz, M. Serda, M. Rejmund, J. Polanski, R. Musiol, The role of oxidative stress in activity of anticancer thiosemicarbazones, Oncotarget. 9 (2018) 17689–17710. https://doi.org/10.18632/oncotarget.24844.

[62] C.S. Birch, N.E. Brasch, A. McCaddon, J.H.H. Williams, A novel role for vitamin B_{12}: Cobalamins are intracellular antioxidants in vitro, Free Radic. Biol. Med. 47 (2009) 184–188. https://doi.org/10.1016/j.freeradbiomed.2009.04.023.

[63] D.V. Beigulenko, N.Yu. Shepeta, K.A. Kochetkov, S.E. Gelperina, Vitamin B_{12} as a Vector for the Transport of Drugs to the Tumor, Macroheterocycles 15 (2022) 6–17. https://doi.org/10.6060/mhc224244k.

[64] A.N.W. Kuda-Wedagedara, J.L. Workinger, E. Nexo, R.P. Doyle, N. Viola-Villegas, ^{89}Zr-Cobalamin PET Tracer: Synthesis, Cellular Uptake, and Use for Tumor Imaging, ACS Omega 2 (2017) 6314–6320. https://doi.org/10.1021/acsomega.7b01180.

[65] P. Ruiz-Sánchez, C. König, S. Ferrari, R. Alberto, Vitamin B_{12} as a carrier for targeted platinum delivery: in vitro cytotoxicity and mechanistic studies, J. Biol. Inorg. Chem. 16 (2011) 33–44. https://doi.org/10.1007/s00775-010-0697-z.

Declaration of Competing Interest

The authors declare the following financial interests/personal relationships which may be considered as potential competing interests: Larissa A. Maiorova reports financial support was provided by Russian Science Foundation. Larissa A. Maiorova reports financial support was provided by Ministry of Science and Higher Education of the Russian Federation. Larissa A. Maiorova reports a relationship with Federal Research Center Computer Science and Control of Russian Academy of Sciences that includes: employment. If there are other authors, they declare that they have no known competing financial interests or personal relationships that could have appeared to influence the work reported in this paper.

Highlights

- Vitamin B_{12} (B_{12}) and its derivatives were successfully encapsulated in BSA particles.
- Aquacobalamin strongly binds with the thiolate residues of the BSA particles.
- The hydrophobic derivative of B_{12} (ACCby) forms nanoparticles in the carriers.
- The BSA with ACCby shows the same neuroprotective effect in vivo as the free drug.
- The promises of using of such systems for nanotheranostics purposes are discussed.